


# Simulation of the fission process of the excited compound nuclei $^{210}\text{Rn}$ and $^{215}\text{Fr}$ produced in fusion reactions within the framework of the modified statistical model

H. Eslamizadeh<sup>\*</sup> and H. Falinejad

*Department of Physics, Faculty of Nano and Bio Science and Technology, Persian Gulf University, 75169 Bushehr, Iran*

 (Received 2 February 2022; accepted 11 March 2022; published 5 April 2022)

In the framework of the modified statistical model there have been simulated fission process of the excited compound nuclei  $^{210}\text{Rn}$  and  $^{215}\text{Fr}$  produced in  $^{16}\text{O} + ^{194}\text{Pt}$  and  $^{19}\text{F} + ^{196}\text{Pt}$  reactions and calculated the evaporation residue cross section, the fission cross section, the fission probability, the average precession neutron multiplicity, the mean fission time, and the anisotropy of fission fragments angular distribution as a function of excitation energy. The classical collective motion of the excited compound nuclei about the ground state, the temperature dependence of the location, the height of fission transition points, and the projection of the total spin of the compound nucleus onto the symmetry axis  $K$  have been considered in the statistical calculations. A constant nuclear dissipation was applied in the statistical calculations. In the statistical calculations, the temperature coefficient of the effective potential  $k$  and the scaling factor of the fission-barrier height  $r_s$  were considered as a free parameter and their magnitudes inferred by fitting measured data on the evaporation residue cross section and the fission cross section for the excited compound nuclei  $^{210}\text{Rn}$  and  $^{215}\text{Fr}$ . It was shown that the results of calculations are in good agreement with the experimental data by using appropriate values for these parameters equal to  $k = 0.0160 \pm 0.0050 \text{ MeV}^{-2}$  and  $r_s = 1.0030 \pm 0.0020$  for  $^{210}\text{Rn}$  and  $k = 0.0065 \pm 0.0040 \text{ MeV}^{-2}$  and  $r_s = 1.0040 \pm 0.0015$  for  $^{215}\text{Fr}$ . Furthermore, by using appropriate values of parameters  $k$  and  $r_s$  have been calculated the average precession neutron multiplicity, the fission probability, the mean fission time, and the anisotropy of fission fragments angular distribution for the nuclei  $^{210}\text{Rn}$  and  $^{215}\text{Fr}$ . Comparison of the theoretical data with the experimental data were shown that the modified statistical model is well able to reproduce different experimental data. Although, at high excitation energies the results of calculations for the anisotropy of fission fragments angular distribution and fission probability are slightly lower than the experimental data.

DOI: [10.1103/PhysRevC.105.044604](https://doi.org/10.1103/PhysRevC.105.044604)

## I. INTRODUCTION

Although the phenomenon of nuclear fission has been discovered since about 80 yr back, the study of fission is still of general interest. Nuclear fission was discovered in December 1938 by chemists Hahn and Strassmann and physicists Meitner and Frisch [1,2]. Shortly after the discovery of nuclear fission, it was interpreted in analogy with the fission of a charged liquid drop. Then, Bohr and Wheeler proposed the standard liquid drop model to describe the fission process of nuclei [3]. According to this model the decay width can be expressed by  $\Gamma = \hbar/\bar{t}$ . Although, the fission lifetime determined from the standard liquid drop model turns out to be too small to allow for the rather large number of experimentally observed light particles that evaporated prior to fission [4]. It should be mentioned that the Bohr and Wheeler description was based on a statistical model according to which fission is governed by the available phase space above the fission barrier. Then, Kramers introduced a picture of fission as a diffusion process across the fission barrier [5]. This description, later refined by Grangé *et al.* [6] with introducing a friction constant which governing the coupling between the equilibrated intrinsic nu-

clear degrees of freedom and the nuclear deformation. The theoretical estimate of the transition-state fission decay width according to Bohr and Wheeler can be given as

$$\Gamma_f = \frac{1}{2\pi} \frac{1}{\rho_{\text{CN}}(E^*)} \int_0^{E^* - B_f} \rho_{\text{sad}}(E^* - B_f - \varepsilon) d\varepsilon, \quad (1)$$

where  $\rho_{\text{CN}}$  and  $\rho_{\text{sad}}$  are the level density of the compound nucleus at the ground and saddle points, respectively.  $B_f$  is the fission barrier height, and  $\varepsilon$  represents the kinetic energy associated with the fission distortion. It should be mentioned that in the limit of a small barrier height or very high excitation energy the temperatures at the ground and saddle points will be equal, and the fission decay width can be given by

$$\Gamma_f = \frac{T}{2\pi} \exp\left(\frac{-B_f}{T}\right), \quad (2)$$

where  $T$  is the temperature of the nucleus. Furthermore, the barrier height can be large enough and the excitation energy low enough such that the temperatures at the ground state and the saddle point are significantly different and so the fission decay width can also be given by

$$\Gamma_f = \frac{T_{\text{sp}}}{2\pi} \exp\left(\frac{-2B_f}{T_{\text{gs}} + T_{\text{sp}}}\right), \quad (3)$$

\*eslamizadeh@pgu.ac.ir

where  $T_{\text{sp}}$  and  $T_{\text{gs}}$  are the temperature of the compound nucleus at the saddle and ground-state points, respectively. In Eq. (1) the density of states can be considered approximately as  $\rho \propto \exp(2\sqrt{aU})$  where  $a$  and  $U$  are the level-density parameter and the thermal excitation energy, respectively. The thermal excitation energy of the system given by  $U = E^* - V(q)$ , where  $E^*$  is the total excitation energy of the system and  $V(q)$  is the potential energy.

Dynamical calculations of the fission rate using the Langevin equation [7] or the Fokker-Planck equation [5] give an asymptotic fission decay width for a system with fixed spin  $K$  about the symmetry axis as follows:

$$\Gamma_f(K) = (\sqrt{1 + \gamma^2} - \gamma) \frac{\hbar\omega_{\text{eq}}}{2\pi} \exp\left(-\frac{B_f}{T}\right), \quad (4)$$

where  $\gamma$  is the dimensionless nuclear viscosity and given by  $\gamma = \beta/2\omega_{\text{sp}}$ ,  $\beta$  is the reduced nuclear dissipation coefficient (ratio of dissipation coefficient to inertia), and  $\omega_{\text{eq}}$ ,  $\omega_{\text{sp}}$  are the curvatures of the potential-energy surface at the equilibrium position and the fission saddle point, respectively.  $B_f$ ,  $\omega_{\text{eq}}$  and  $\omega_{\text{sp}}$  are all assumed functions of  $K$ .

After Bohr and Wheeler model, many statistical and dynamical model codes were proposed to describe fission process of nuclei (see, for example, Refs. [8–29]). It should be mentioned that in many statistical codes that introduced to describe the fission process missing three pieces of physics as first pointed out by Lestone and McCalla in Ref. [30]. These key pieces of physics are the determination of the total level density of the compound system taking into account the collective motion of the system about the ground-state position, the calculation of the location and height of fission saddle points as a function of excitation energy and the incorporation of the orientation ( $K$  state) degree of freedom. It should be mentioned that in many statistical model codes (see, for example, Refs. [12–16]) authors have used the ratio of the level-density parameters at saddle and equilibrium deformations,  $a_{\text{sp}}/a_{\text{eq}}$ , and a scaling of the fission barrier heights  $f_B$ , which can be adjusted to reproduce different experimental data. Although, the fission process cannot be accurately modeled as a function of the excitation energy by using a fixed value of  $a_{\text{sp}}/a_{\text{eq}}$  and the spin dependence of the  $T = 0$  fission barriers [30] ( $T$  is the temperature). Lestone and McCalla in Ref. [30] introduced a modified statistical model (MSM) and in this model, they considered the above missing three pieces of physics and also other parameters as free parameters which perform similar roles as  $a_{\text{sp}}/a_{\text{eq}}$  and  $f_B$ . They considered the temperature coefficient in the effective potential formula  $k$ , and a scaling of the modified liquid drop model (MLDM) radii from their default values to calculate the surface and Coulomb energies with the parameter  $r_s$ . The surface energy is proportional to the square of  $r_s$ , while the Coulomb energy is inversely proportional to  $r_s$ . A value  $r_s = 1$  is the standard MLDM with fission-barrier heights in agreement with the finite range liquid drop model. Raising  $r_s$  above one decreases the Coulomb energy and increases the surface energy. This

cases the fission barriers to increase. It should be stressed that the advantage of using  $r_s$  instead of  $f_B$  is that the curvature at the ground states and the fission transition points, the barrier locations and heights are all being determined in a self-consistent manner as a function of spin  $J$ , projection of spin about the symmetry axis of the nucleus  $K$ , and temperature of the nucleus. The main purpose of this research is to present the ability of MSM to reproduce different features of the fission process of the excited nuclei  $^{210}\text{Rn}$  and  $^{215}\text{Fr}$  produced in  $^{16}\text{O} + ^{194}\text{Pt}$  and  $^{19}\text{F} + ^{196}\text{Pt}$  reactions, respectively.

The present paper has been arranged as follows. In Sec. II, we describe the model and basic equations. The results of calculations are presented in Sec. III. Finally, the concluding remarks are given in Sec. IV.

## II. DETAILS OF THE MODEL

In the framework of the MSM the time evolution of an excited compound nucleus produced in a fusion reaction is followed over small time steps. At each time step, evaporation of precession particles and the  $\gamma$  particle from a compound nucleus are taken into account by using a Monte Carlo simulation technique. The loss of spin for a compound nucleus is taken into account by assuming that each neutron, proton or  $\gamma$  quanta carries away  $1\hbar$  whereas the  $\alpha$  particle carries away  $2\hbar$ . The compound nucleus can follow various decay routes depending upon the relative probabilities of different decay channels. It should be stressed that one can consider fission along with emission of neutrons, protons,  $\alpha$  particles, and  $\gamma$  rays as the decay channels of a compound nucleus. A compound nucleus can either undergo fission with or without preceding evaporation of particles and  $\gamma$  rays or reduce to an evaporation residue. In the calculations based on the statistical model, we obtain the decay widths for particle emission and fission width and the kind of decay is selected in terms of a standard Monte Carlo cascade procedure with considering the weights of  $\Gamma_v/\Gamma_{\text{tot}}$  with ( $v = \text{fission}, n, p, \alpha, \gamma$ ) and  $\Gamma_{\text{tot}} = \sum_v \Gamma_v$ . The final results for different observables can be obtained as averages over a large ensemble of events.

It should be noted that the potential energy, level density, the evaporation, and fission widths depend on the spin of the compound nucleus. The spin of a compound nucleus can be sampled from the spin distribution. The spin distribution of compound nuclei  $d\sigma(J)/dJ$ , produced in fusion reactions can be determined by [31]

$$\frac{d\sigma(J)}{dJ} = \frac{2\pi}{K^2} \frac{2J + 1}{1 + \exp\left(\frac{J - J_c}{\delta J}\right)}, \quad (5)$$

here  $K$  is wave number,  $J_c$  is the critical spin and  $\delta J$  is the diffuseness parameter. The parameters  $J_c$  and  $\delta J$  can be determined by [31]

$$J_c = \sqrt{A_p A_T / A_{\text{CN}}} (A_p^{1/3} + A_T^{1/3}) (0.33 + 0.205 \sqrt{E_{\text{c.m.}} - V_c}), \quad (6)$$

and

$$\delta J = \begin{cases} (A_p A_T)^{3/2} \times 10^{-5} [1.5 + 0.02(E_{\text{c.m.}} - V_c - 10)] & \text{for } E_{\text{c.m.}} > V_c + 10, \\ (A_p A_T)^{3/2} \times 10^{-5} [1.5 - 0.04(E_{\text{c.m.}} - V_c - 10)] & \text{for } E_{\text{c.m.}} < V_c + 10, \end{cases} \quad (7)$$

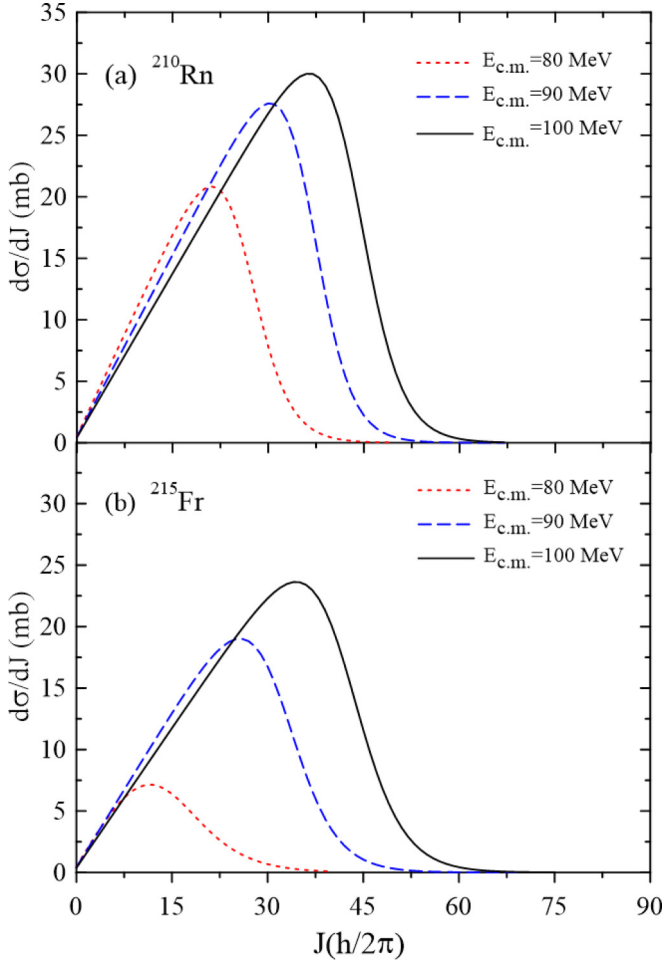


FIG. 1. The spin distributions calculated for the compound nuclei (a)  $^{210}\text{Rn}$  and (b)  $^{215}\text{Fr}$  produced in  $^{16}\text{O} + ^{194}\text{Pt}$  and  $^{19}\text{F} + ^{196}\text{Pt}$  reactions at  $E_{\text{c.m.}} = 80, 90,$  and  $100$  MeV.

when  $0 < E_{\text{c.m.}} - V_c < 120$  MeV center-of-mass (c.m.); and when  $E_{\text{c.m.}} - V_c > 120$  MeV the term in the last brackets is set equal to 2.5. Figures 1(a) and 1(b) show the spin distributions calculated for the compound nuclei  $^{210}\text{Rn}$  and  $^{215}\text{Fr}$  produced in  $^{16}\text{O} + ^{194}\text{Pt}$  and  $^{19}\text{F} + ^{196}\text{Pt}$  reactions, for example, for projectile energies  $E_{\text{c.m.}} = 80, 90,$  and  $100$  MeV.

It is clear from Figs. 1(a) and 1(b) that at higher center-of-mass energies of the projectiles the compound nuclei formed with a larger value of spins.

The potential-energy  $V$  can be obtained from the MLDM. The MLDM uses a family of axially symmetric and mass symmetric shapes. These shapes define the Coulomb, surface, and rotational energies of nuclei as a function of a single deformation parameter  $q = r/R_0$ , where  $r$  is the distance between the centers of masses of the future fission fragments and  $R_0$  is the radius of the spherical nucleus. In the MLDM, the potential energy of a nucleus can be written as [32,33]

$$V(q, A, Z, J, K) = B_s(q)E_s^0(Z, A) + B_c(q)E_c^0(Z, A) + E_{\text{rot.}}, \quad (8)$$

where  $B_c(q)$  and  $B_s(q)$  are Coulomb and surface energy terms, respectively.  $E_s^0$  and  $E_c^0$  are, respectively, the surface and Coulomb energies of the corresponding spherical system as determined by Myers and Swiatecki [34,35]. In Eq. (8)  $E_{\text{rot.}}$  is the rotational energy and can be determined by

$$E_{\text{rot.}} = \frac{[J(J+1) - K^2]\hbar^2}{I_{\perp}(q)\frac{4}{5}MR_0^2 + 8Ma^2} + \frac{K^2\hbar^2}{I_{\parallel}(q)\frac{4}{5}MR_0^2 + 8Ma^2}, \quad (9)$$

where  $K$  is the projection of  $J$  on the symmetry axis of the nucleus,  $M$  is the mass of the system,  $R_0 = 1.2249A^{1/3}$  (fm) and  $a = 0.6$  (fm).  $I_{\perp}$  and  $I_{\parallel}$  are the momenta of inertia with respect to the axes perpendicular and parallel to the symmetry axis of the fissioning nucleus.

It should be noted that the Bohr-Wheeler fission decay width given by Eq. (2) was obtained assuming that the level-density parameter is independent of the nuclear shape. Although, this equation by using a deformation dependence of the level density of the form

$$a(q) = a_v A + a_s A^{2/3} B_s(q), \quad (10)$$

can be written as

$$\Gamma_f \approx \frac{T}{2\pi} \exp(B_{\text{eff}}/T). \quad (11)$$

In Eq. (10)  $A$  is the mass number of the compound nucleus, and  $B_s(q)$  is the surface energy in the liquid drop model. The values of the parameters  $a_v = 0.073$  and  $a_s = 0.095$  MeV $^{-1}$  in Eq. (10) are taken from the work of Ignatyuk *et al.* [36]. In Eq. (11)  $B_{\text{eff}}$  is the effective potential barrier height and can be given by

$$B_{\text{eff}} = B_f - \Delta a T^2, \quad (12)$$

where  $\Delta a$  is equal to the difference in the level-density parameter at the saddle point and the equilibrium position. It should be noted that at finite temperature the driving force is the free energy [37],

$$F = E^* - TS(q, E_{\text{int.}}), \quad (13)$$

where  $S$  is the entropy. If the level-density parameter is a function of nuclear deformation, then the locations of equilibrium points will be a function of excitation energy and can be defined by the equilibrium points in the entropy or level-density parameter as a function of deformation,

$$\left( \frac{\partial S(q)}{\partial q} \right)_{E_{\text{int.}}} \approx \left( \frac{\partial (2\sqrt{a(q)E_{\text{int.}}})}{\partial q} \right)_{E_{\text{int.}}} = 0, \quad (14)$$

and not as the equilibrium points in the  $T = 0$  potential energy. Searching for the equilibrium points in the entropy is the same as searching for the equilibrium points in a temperature-dependent effective potential energy [38],

$$V_{\text{eff}}(q, A, Z, J, K, T) = V(q, A, Z, J, K) - \Delta a(q)T^2. \quad (15)$$

If the level-density parameter is assumed to be as Eq. (10), then the effective potential can be obtained using a  $(1 - kT^2)$

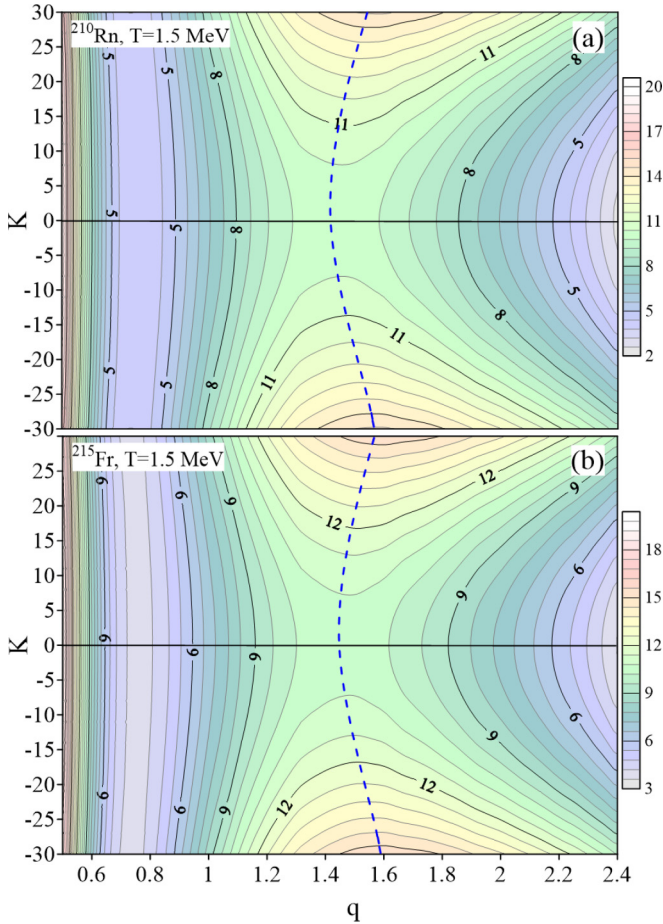


FIG. 2. The effective potential for the compound nuclei (a)  $^{210}\text{Rn}$  and (b)  $^{215}\text{Fr}$  as a function of the coordinates  $q$  and  $K$  at  $T = 1.5$  MeV and  $J = 30\hbar$ . The numbers at the contour lines represent the effective potential energy values in MeV. The dashed line curves show the dependence of saddle point deformations on  $K$ .

dependence of the surface energy,

$$V_{\text{eff}}(q, A, Z, J, K, T) = B_s(q)E_s^0(Z, A)(1 - kT^2) + B_c(q)E_c^0(Z, A) + E_{\text{rot}}, \quad (16)$$

where  $k = c_s A^{2/3} / E_s^0$ . Töke and Swiatecki [39] obtain  $c_s \approx 0.27$ , and other estimates of  $c_s$  give values of  $k$  that range from 0.007 to 0.022 MeV $^{-2}$  [36,40–43]. It should be stressed that  $c_s$  is very sensitive to the assumed properties of nuclear matter and to other approximations [43]. Figures 2(a) and 2(b) show the effective potential calculated for the compound nuclei  $^{210}\text{Rn}$  and  $^{215}\text{Fr}$  as a function of the coordinates  $q$  and  $K$  at  $T = 1.5$  MeV and  $J = 30\hbar$ . It can be seen from Figs. 2(a) and 2(b) that the inclusion of the  $K$  coordinate changes not only the fission barrier height, but it affects also the saddle point configuration. It is also clear from Figs. 2(a) and 2(b) that for a given value of spin the height of the fission barrier increases with increasing the value of  $K$  and, consequently, increases the number of evaporated prescission particles.

The particle emission width of a particle of kind  $v$  can be determined as Ref. [44],

$$\Gamma_v = (2s_v + 1) \frac{m_v}{\pi^2 \hbar^2 \rho_c(E_{\text{int.}})} \times \int_0^{E_{\text{int.}} - B_v} d\varepsilon_v \rho_R(E_{\text{int.}} - B_v - \varepsilon_v) \varepsilon_v \sigma_{\text{inv.}}(\varepsilon_v), \quad (17)$$

here  $s_v$  is the spin of the emitted particle  $v$ ,  $m_v$  is its reduced mass with respect to the residual nucleus,  $\varepsilon$  is the energy of the emitted particle,  $E_{\text{int.}}$  is the intrinsic excitation energy of the parent nucleus, and  $B_v$  is liquid drop binding energies of the emitted particle  $v$ .  $\rho_c(E_{\text{int.}})$  and  $\rho_R(E_{\text{int.}} - B_v - \varepsilon_v)$  are the level densities of the compound and residual nuclei. The inverse cross sections can be written as [44]

$$\sigma_{\text{inv.}}(\varepsilon_v) = \begin{cases} \pi R_v^2 (1 - V_v/\varepsilon_v) & \text{for } \varepsilon_v > V_v, \\ 0 & \text{for } \varepsilon_v < V_v, \end{cases} \quad (18)$$

with

$$R_v = 1.21 [(A - A_v)^{1/3} + A_v^{1/3}] + (3.4/\varepsilon_v^{1/2}) \delta_{v,n}, \quad (19)$$

where  $A_v$  is the mass number of the emitted particle  $v = n, p, \alpha$  and  $\delta_{vn}$  is the  $\delta$  function. The barriers for the charged particles are

$$V_v = [(Z - Z_v)Z_v K_v] / (R_v + 1.6), \quad (20)$$

with  $K_v = 1.32$  for  $\alpha$  and 1.15 for the proton.

The  $\gamma$ -ray decay width at each time step is calculated as in Ref. [45],

$$\Gamma_\gamma \cong \frac{3}{\rho_c(E_{\text{int.}})} \int_0^{E_{\text{int.}}} d\varepsilon \rho_c(E_{\text{int.}} - \varepsilon) f(\varepsilon), \quad (21)$$

here  $\varepsilon$  is the energy of the emitted  $\gamma$  ray and  $f(\varepsilon)$  is calculated by

$$f(\varepsilon) = \frac{4}{3\pi} \frac{e^2}{\hbar c} \frac{1 + \eta NZ}{mc^2} \frac{\Gamma_G \varepsilon^4}{(\Gamma_G \varepsilon)^2 + (\varepsilon^2 - E_G^2)^2}, \quad (22)$$

with  $E_G = 80A^{-1/3}$ ,  $\Gamma_G = 5$  MeV, and  $\eta = 0.75$  [46],  $E_G$  and  $\Gamma_G$  are the position and width of the giant dipole resonance, respectively.

The fission width for a system with fixed spin  $K$  about the symmetry axis can be determined by Eq. (4). By assuming axially symmetric shapes for nuclei the full fission decay width can be obtained by summing over all possible  $K$  s [32],

$$\Gamma_f = \frac{\sum_{K=-J}^J P(K) \Gamma_f(K)}{\sum_{K=-J}^J P(K)}, \quad (23)$$

where  $P(K)$  is the probability that the system is in a given  $K$  and it can be expressed as follows:

$$P(K) = \frac{T}{\hbar \omega_{\text{eq}}} \exp\left(-\frac{V_{\text{eq}}}{T}\right), \quad (24)$$

$V_{\text{eq}}$  is the potential energy at the equilibrium position as a function of  $K$ .

It should be stressed that the level density is a key physical quantity in the calculations because it comes in all the disintegration widths. In the framework of the MSM the level density

of a spherical compound nucleus as a function of the total excitation energy  $E^*$ , the total spin  $J$ , and the projection of spin about the symmetry axis of the nucleus  $K$  is determined by [37]

$$\rho_{\text{sph}}(E^*, J, K) \propto \frac{\exp(2\sqrt{aE_{\text{int}}})}{E_{\text{int}}^2}, \quad (25)$$

where  $E_{\text{int}}$  is intrinsic energy. The intrinsic energy for a rotating system can be given by  $E_{\text{int}} = E^* - V(q) - E_{\text{rot}}$ . For the spherically symmetric case the rotational energy is obviously independent of  $K$ , and the level density can be given as

$$\begin{aligned} \rho_{\text{sph}}(E^*, J) &= \sum_{K=-J}^J \rho_{\text{sph}}(E^*, J, K) \\ &\propto (2J+1) \frac{\exp(2\sqrt{aE_{\text{int}}})}{E_{\text{int}}^2}. \end{aligned} \quad (26)$$

In Eq. (26) the  $2J+1$  factor is associated with the complete freedom of the orientation degree of freedom in the case of a spherical compound nucleus. For an arbitrary deformation, a multiplication factor associated with the orientation degree of freedom can be considered for Eq. (26) as follows:

$$f = \sum_{K=-J}^J \exp\left(\frac{-K^2}{2K_0^2(q)}\right) \approx K_0 \sqrt{2\pi} \operatorname{erf}\left(\frac{2J+1}{2\sqrt{2}K_0(q)}\right), \quad (27)$$

where

$$K_0^2(q) = TI_{\text{eff}}(q)/\hbar^2. \quad (28)$$

The inverse of the effective moment of inertia can be determined by  $I_{\text{eff}}^{-1} = I_{\parallel}^{-1} - I_{\perp}^{-1}$ .

The total fusion cross section is usually calculated from

$$\sigma_{\text{Fus}} = \sum_J \frac{d\sigma_{\text{Fus}}(J)}{dJ}, \quad (29)$$

where, the spin distribution of the compound nucleus can be considered by Eq. (5). The fission cross section can also be determined in terms of the fusion cross section as follows:

$$\sigma_{\text{Fiss}} = \sum_J \sigma_{\text{Fus}}(J) \frac{\Gamma_f}{\Gamma_{\text{tot}}}. \quad (30)$$

At a given beam energy  $E$ , the total evaporation residue cross section can be obtained by summing of the cross sections from each  $J$ , these being the products of the capture cross sections, and the probabilities of surviving fission  $[1 - P_f(J, E^*)]$ ,

$$\sigma_{Er}(E) = \pi \lambda^2 \sum_{J=0} (2J+1) T_J [1 - P_f(J, E^*)], \quad (31)$$

where  $T_J$  is the transmission coefficient for  $J$ th partial wave and  $P_f$  is fission probability of the compound nucleus.

In the MSM, one can use the saddle point transition model [47–49] to analyze the fission fragment angular distributions. The fission fragment angular distributions can be determined by three quantum numbers:  $J$ ,  $M$ ,  $K$ , where  $J$  is the spin of a compound nucleus,  $M$  is the projection of  $J$  on the axis of

the projectile ion beam, and  $K$  is the projection of  $J$  on the symmetry axis of the nucleus. In the case of fusion of spinless ions,  $M = 0$ . Then at fixed values of  $J$  and  $K$ , the angular distribution can be determined as follows:

$$W(\theta, J, K) = (J+1/2) |d_{M=0,K}^J(\theta)|^2, \quad (32)$$

where  $\theta$  is the angle between the nuclear symmetry axis and the beam axis and  $d_{M=0,K}^J(\theta)$  is the Wigner rotation function [47]. It should be mentioned that in the case of heavy-ion-induced fission reactions, the spin of compound nucleus is usually much larger than the ground-state spins of the target and projectile and is perpendicular to the beam axis, so in this case also  $M = 0$ . At high values of  $J$ ,  $W(\theta, J, K)$  can be approximated as

$$W(\theta, J, K) = \frac{J+1/2}{\pi} [(J+1/2)^2 \sin^2 \theta - K^2]^{1/2}. \quad (33)$$

The fission fragments angular distribution can be determined by averaging Eq. (33) over the quantum numbers  $J$  and  $K$  as follows:

$$W(\theta) = \sum_{J=0}^{\infty} \sigma_J \sum_{K=-J}^J P(K) W(\theta, J, K), \quad (34)$$

where  $\sigma_J$  and  $P(K)$  are the distributions of compound nuclei with respect to the total spin and its projection, respectively [49]. It can be shown that the anisotropy of fission fragment angular distribution can be given by the following approximate relation:

$$\frac{\langle W(180^\circ) \rangle}{\langle W(90^\circ) \rangle} = 1 + \frac{\langle J^2 \rangle}{4K_0^2}, \quad (35)$$

where the variance of  $K$  distribution  $K_0$ , is given by the expression,

$$K_0^2 = (T/\hbar^2) I_{\text{eff}}. \quad (36)$$

### III. RESULTS AND DISCUSSIONS

In the framework of the MSM have been simulated fission process of the excited compound nuclei  $^{210}\text{Rn}$  and  $^{215}\text{Fr}$  produced in  $^{16}\text{O} + ^{194}\text{Pt}$  and  $^{19}\text{F} + ^{196}\text{Pt}$  reactions, respectively. The evaporation residue cross section, the fission cross section, the fission probability, the anisotropy of fission fragments angular distribution, the average pre-scission neutron multiplicity, and the mean fission time have been calculated for the excited compound nuclei  $^{210}\text{Rn}$  and  $^{215}\text{Fr}$ . In the statistical calculations, the reduced nuclear dissipation coefficient is set as  $3 \times 10^{21} \text{s}^{-1}$ , a value that is consistent with experimental and theoretical estimates [31,50,51]. In the present calculations, the parameters  $k$  and  $r_s$  are adjusted to reproduce a single residue and fission cross sections. Figures 3(a), 3(b), 4(a), and 4(b) show the results of calculations for the residue and fission cross sections for the excited compound nuclei  $^{210}\text{Rn}$  and  $^{215}\text{Fr}$ . It can be seen from Figs. 3(a), 3(b), 4(a), and 4(b) that the results of the calculations are in good agreement with the experimental data by using values of  $k = 0.0160 \pm 0.0050 \text{ MeV}^{-2}$  and  $r_s = 1.0030 \pm 0.0020$  for  $^{210}\text{Rn}$  and  $k = 0.0065 \pm 0.0040 \text{ MeV}^{-2}$  and  $r_s = 1.0040 \pm 0.0015$  for  $^{215}\text{Fr}$ .

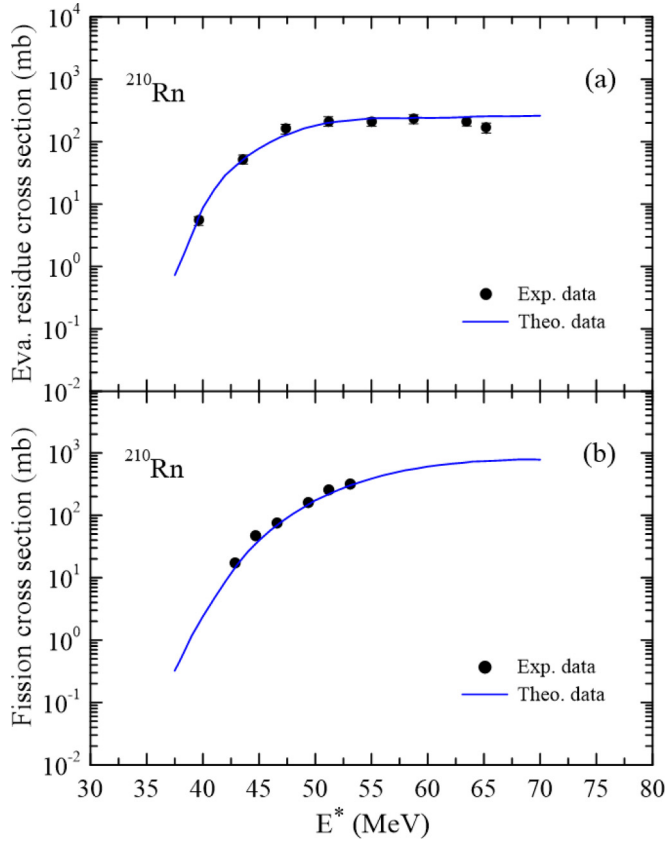


FIG. 3. The results of the evaporation residue cross section and the fission cross section for the compound nucleus  $^{210}\text{Rn}$ , calculated with considering  $k = 0.0160 \pm 0.0050 \text{ MeV}^{-2}$  and  $r_s = 1.0030 \pm 0.0020$ . The solid circles are experimental data [52,53].

Figures 5(a) and 5(b) show the results of calculations for the average pre-fission neutron multiplicities for the excited compound nuclei  $^{210}\text{Rn}$  and  $^{215}\text{Fr}$ . It can be seen from Figs. 5(a) and 5(b) that by considering appropriate values for the parameters  $k$  and  $r_s$  where obtained in the analyze of residue and fission cross sections can be satisfactorily reproduced the experimental data on the average pre-fission neutron multiplicities for the excited compound nuclei  $^{210}\text{Rn}$  and  $^{215}\text{Fr}$ . It can be seen from Figs. 5(a) and 5(b) that at lower and intermediate excitation energies the values of the average pre-fission neutron multiplicities calculated with considering appropriate values for the parameters  $k$  and  $r_s$  are close to the experimental data, although at higher excitation energies the calculated data are slightly lower than the experimental data. This is probably due to the compound nucleus at higher excitation energy is formed with a larger value of spin and temperature. Thus, the fission barrier height will be reduced, and, therefore, the neutron widths are comparable to the fission widths, and so the calculations data for the pre-fission neutron multiplicities are slightly lower than the experimental data. It should be mentioned that in simulation of the fission process of a compound nucleus, it is very important to consider the effect of the parameters  $k$  and  $r_s$ . It can be investigated, for example, by estimation of the pre-fission neutron multiplicity for the excited compound nuclei  $^{210}\text{Rn}$  and  $^{215}\text{Fr}$

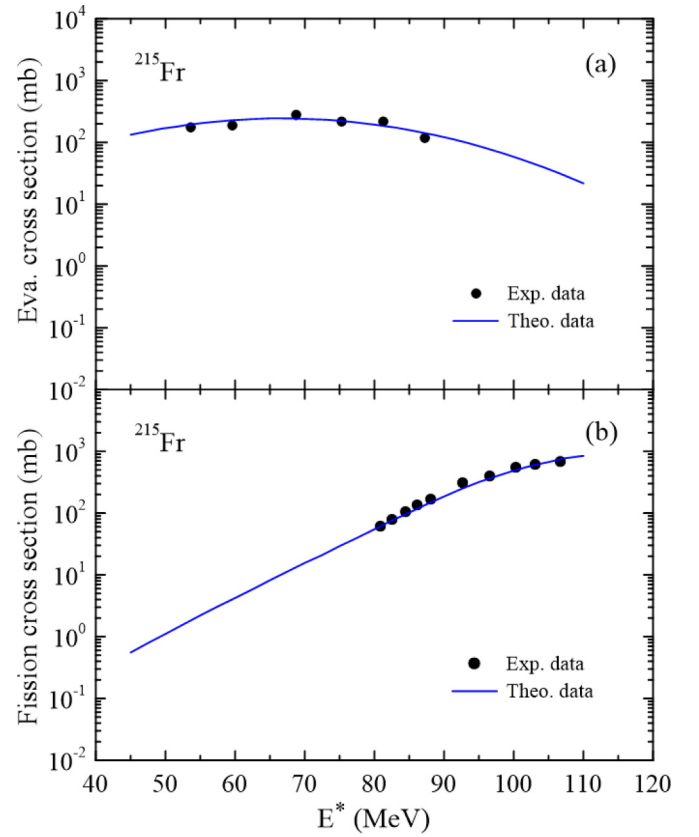


FIG. 4. The results of the evaporation residue cross section and the fission cross section for the compound nucleus  $^{215}\text{Fr}$ , calculated with considering  $k = 0.0065 \pm 0.0040 \text{ MeV}^{-2}$  and  $r_s = 1.0040 \pm 0.0015$ . The solid circles are experimental data [54,55].

with considering  $k = 0$  and  $r_s = 1$ . The results of calculations for neutron multiplicities by using  $k = 0$  and  $r_s = 1$  are also included in Figs. 5(a) and 5(b). It is clear from Figs. 5(a) and 5(b) that by using  $k = 0$  and  $r_s = 1$  the results of calculations for pre-fission neutron multiplicities decreased for  $^{210}\text{Rn}$  and  $^{215}\text{Fr}$ .

Figure 6 shows the results of anisotropy of the fission fragment angular distribution as a function of energy for the excited compound nucleus  $^{210}\text{Rn}$  and Figs. 7(a) and 7(b) show the results of the fission fragment angular distribution as a function of scattering angle at bombarding energy  $E_{\text{lab}} = 89.80$  and  $E_{\text{lab}} = 104.90 \text{ MeV}$  for the excited compound nuclei (a)  $^{210}\text{Rn}$  and (b)  $^{215}\text{Fr}$ .

It can be seen from Figs. 6 and 7 that the difference between the results calculated with MSM and experimental data are small, although at higher excitation energies the calculated data are slightly lower than the experimental data.

In the present research the fission probability has been also calculated for the excited compound nucleus  $^{210}\text{Rn}$  with considering  $k = 0.0160 \pm 0.0050 \text{ MeV}^{-2}$  and  $r_s = 1.0030 \pm 0.0020$ . Figure 8 shows the fission probability for the compound nucleus  $^{210}\text{Rn}$  as a function of excitation energy. It can also be seen from Fig. 8 that at higher excitation energies the results of calculations lie slightly below the experimental data.

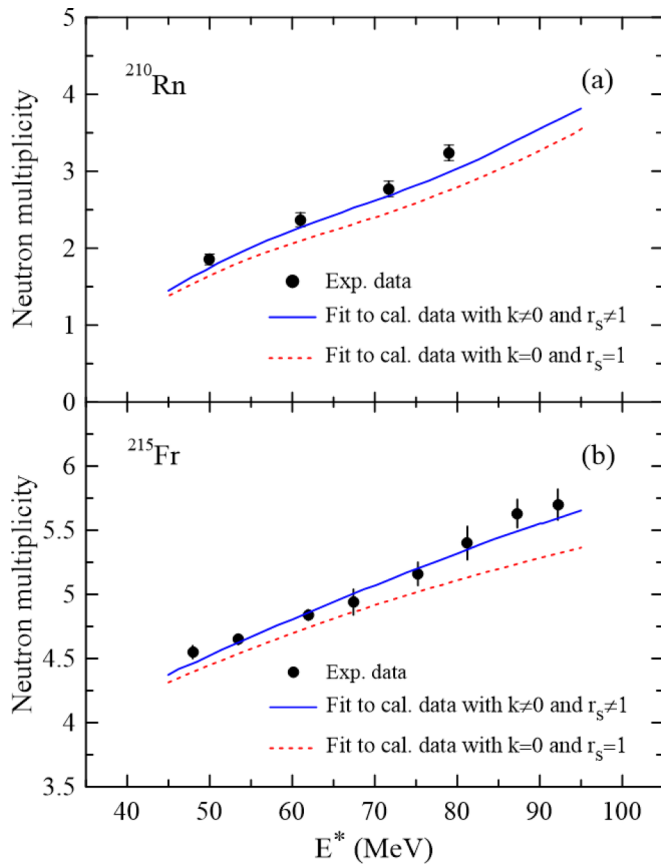


FIG. 5. The results of the preffission neutron multiplicities as a function of excitation energy for the excited compound nuclei (a)  $^{210}\text{Rn}$  and (b)  $^{215}\text{Fr}$  calculated with considering appropriate values for the parameters  $k$  and  $r_s$  (solid lines). The dotted lines show the results of the preffission neutron multiplicities calculated with considering  $k = 0$  and  $r_s = 1$ . The solid circles are experimental data [56,57].

Finally, in the present investigation the mean fission time have been calculated for the excited compound nuclei  $^{210}\text{Rn}$  and  $^{215}\text{Fr}$ . Figure 9 shows the results of the mean fission time as a function of excitation energy for the excited compound

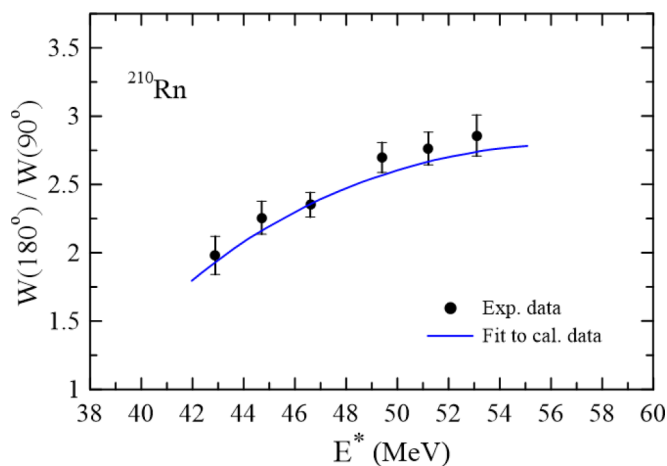


FIG. 6. The results of anisotropy of the fission fragment angular distribution as a function of excitation energy for the compound nucleus  $^{210}\text{Rn}$ . The solid circles are experimental data [53].

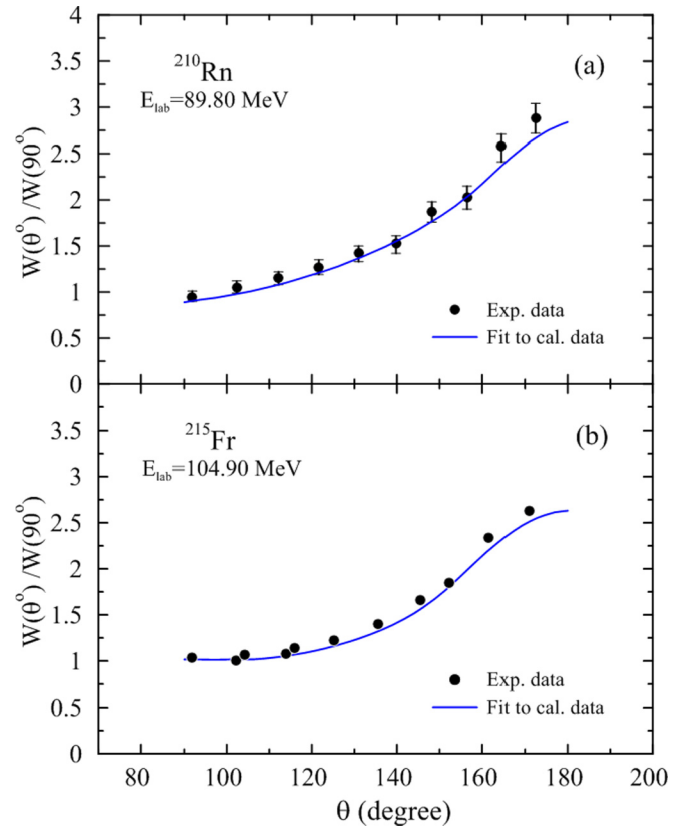


FIG. 7. The results of fission fragment angular distributions as a function of scattering angle at bombarding energies  $E_{\text{lab}} = 89.80$  and  $E_{\text{lab}} = 104.90$  MeV for the excited compound nuclei (a)  $^{210}\text{Rn}$  and (b)  $^{215}\text{Fr}$ . The solid circles are experimental data [53,58].

nuclei  $^{210}\text{Rn}$  and  $^{215}\text{Fr}$ . It can be seen from Fig. 9 that the mean fission time decreases rapidly with increasing excitation energy.

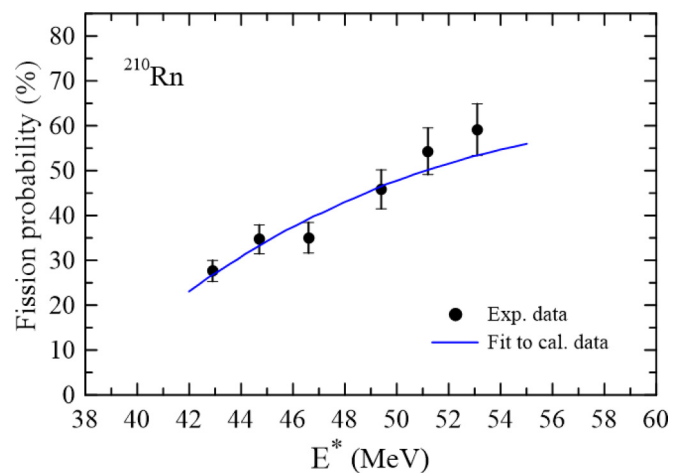


FIG. 8. The results of fission probability as a function of excitation energy for the compound nucleus  $^{210}\text{Rn}$ . The solid circles are experimental data [53].

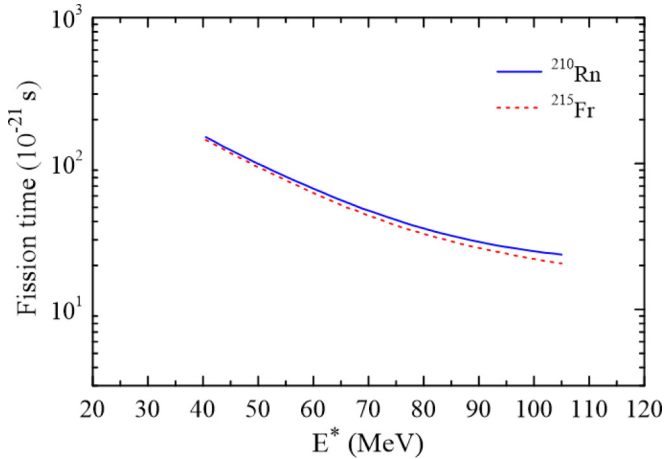


FIG. 9. The results of the mean fission time for the excited compound nuclei  $^{210}\text{Rn}$  and  $^{215}\text{Fr}$  calculated in the framework of the MSM.

#### IV. CONCLUSIONS

In the framework of the modified statistical model have been calculated the evaporation residue cross section, the fission cross section, the fission probability, the average precession neutron multiplicity, the mean fission time, and the anisotropy of fission fragments angular distribution as a function of excitation energy for the excited compound nuclei  $^{210}\text{Rn}$  and  $^{215}\text{Fr}$  produced in fusion reaction. In the statistical

calculations, the temperature coefficient of the effective potential  $k$  and the scaling factor of the fission-barrier height,  $r_s$ , were considered as a free parameter and their magnitudes inferred by fitting measured data on the evaporation residue cross section and the fission cross section. It was shown that the results of calculations are in good agreement with the experimental data by using appropriate values for these parameters equal to  $k = 0.0160 \pm 0.0050 \text{ MeV}^{-2}$  and  $r_s = 1.0030 \pm 0.0020$  for  $^{210}\text{Rn}$  and  $k = 0.0065 \pm 0.0040 \text{ MeV}^{-2}$  and  $r_s = 1.0040 \pm 0.0015$  for  $^{215}\text{Fr}$ . In the present investigation, by using appropriate values of parameters  $k$  and  $r_s$  have also been calculated the fission probability, the average precession neutron multiplicity, the mean fission time, and the anisotropy of fission fragments angular distribution for the compound nuclei  $^{210}\text{Rn}$  and  $^{215}\text{Fr}$ . Comparison of the theoretical data with the experimental data was shown that the modified statistical model is well able to reproduce these experimental data for the nuclei  $^{210}\text{Rn}$  and  $^{215}\text{Fr}$  by using appropriate values for the parameters  $k$  and  $r_s$ . Although, at high excitation energies the results of calculations for the anisotropy of fission fragments angular distribution and fission probability are slightly lower than the experimental data.

#### ACKNOWLEDGMENTS

We thank the anonymous referee for comments and suggestions, which led to a significantly improved version of this paper. Support from the Research Committee of the Persian Gulf University was greatly acknowledged.

- [1] O. Hahn and F. Strassmann, *Sci. Nat.* **27**, 163 (1939).
- [2] L. Meitner and O. R. Frisch, *Nature (London)* **143**, 471 (1939).
- [3] N. Bohr and J. A. Wheeler, *Phys. Rev.* **56**, 426 (1939).
- [4] M. Thoennessen and G. F. Bertsch, *Phys. Rev. Lett.* **71**, 4303 (1993).
- [5] H. A. Kramers, *Physica* **7**, 284 (1940).
- [6] P. Grangé, J. Q. Li, and H. A. Weidenmüller, *Phys. Rev. C* **27**, 2063 (1983).
- [7] D. Boilley, E. Suraud, Y. Abe, and S. Ayik, *Nucl. Phys. A* **556**, 67 (1993).
- [8] H. Eslamizadeh and H. Razazzadeh, *Phys. Lett. B* **777**, 265 (2018).
- [9] M. D. Usang, F. A. Ivanyuk, C. Ishizuka, and S. Chiba, *Phys. Rev. C* **96**, 064617 (2017).
- [10] M. D. Usang, F. A. Ivanyuk, C. Ishizuka, and S. Chiba, *Sci. Rep.* **9**, 1525 (2019).
- [11] H. Eslamizadeh and E. Ahadi, *Phys. Rev. C* **96**, 034621 (2017).
- [12] A. Gavron, *Phys. Rev. C* **21**, 230 (1980).
- [13] M. Blann and T. A. Komoto, Lawrence Livermore National Laboratory Report No. UCID 19390 (1982).
- [14] M. Blann and J. Bisplinghoff, Lawrence Livermore National Laboratory Report No. UCID 19614 (1982).
- [15] H. Rossner, D. Hilscher, D. J. Hinde, B. Gebauer, M. Lehmann, M. Wilpert, and E. Mordhorst, *Phys. Rev. C* **40**, 2629 (1989).
- [16] J. P. Lestone, J. R. Leigh, J. O. Newton, D. J. Hinde, J. X. Wei, J. X. Chen, S. Elström, and M. Zielinska-Pfabé, *Nucl. Phys. A* **559**, 277 (1993).
- [17] H. Eslamizadeh, *Int. J. Mod. Phys. E* **24**, 1550052 (2015).
- [18] H. Eslamizadeh, *Int. J. Mod. Phys. E* **21**, 1250008 (2012).
- [19] N. Wang and W. Ye, *Phys. Rev. C* **103**, 024611 (2021).
- [20] N. Wang and W. Ye, *Phys. Rev. C* **97**, 014603 (2018).
- [21] H. Eslamizadeh and F. Bagheri, *Chin. Phys. C* **41**, 044101 (2017).
- [22] H. Eslamizadeh, *Pramana* **80**, 621 (2013).
- [23] V. T. Maslyuk, O. O. Parlag, M. I. Romanyuk, O. I. Lendyel, and T. J. Marinetc, *Europhys. Lett.* **119**, 12001 (2017).
- [24] N. Vonta, G. A. Souliotis, M. Veselsky, and A. Bonasera, *Phys. Rev. C* **92**, 024616 (2015).
- [25] V. Y. Denisov, T. O. Margitych, and I. Y. Sedykh, *Nucl. Phys. A* **958**, 101 (2017).
- [26] K. Schmidt and B. Jurado, *Rep. Prog. Phys.* **81**, 106301 (2018).
- [27] H. Eslamizadeh, *Pramana* **78**, 231 (2012).
- [28] I. I. Gontchar, N. A. Ponomarenko, V. V. Turkin, and L. A. Litnevsky, *Phys. At. Nucl.* **67**, 2080 (2004).
- [29] H. Eslamizadeh and M. Soltani, *Ann. Nucl. Energy* **80**, 261 (2015).
- [30] J. P. Lestone and S. G. McCalla, *Phys. Rev. C* **79**, 044611 (2009).
- [31] P. Fröbrich and I. I. Gontchar, *Phys. Rep.* **292**, 131 (1998).
- [32] J. P. Lestone, *Phys. Rev. C* **59**, 1540 (1999).
- [33] J. P. Lestone, *Phys. Rev. C* **51**, 580 (1995).
- [34] W. D. Myers and W. J. Swiatecki, *Nucl. Phys.* **81**, 1 (1966).
- [35] W. D. Myers and W. J. Swiatecki, *Ark. Fys.* **36**, 343 (1967).
- [36] A. V. Ignatyuk, M. G. Itkis, V. N. Okolovich, G. N. Smirenkin, and A. S. Tishin, *Yad. Fiz.* **21**, 1185 (1975).



- [37] A. Bohr and B. R. Mottelson, *Nuclear Structure Vol. I and II*, (W. A. Benjamin, New York/London, 1975).
- [38] I. I. Gontchar, P. Fröbrich, and N. I. Pischasov, *Phys. Rev. C* **47**, 2228 (1993).
- [39] J. Töke and W. J. Swiatecki, *Nucl. Phys. A* **372**, 141 (1981).
- [40] W. Reisdorf, *Z. Phys. A: At. Nucl.* **300**, 227 (1981).
- [41] M. Prakash, J. Wambach, and Z. Y. Ma, *Phys. Lett. B* **128**, 141 (1983).
- [42] S. Shlomo, *Nucl. Phys. A* **539**, 17 (1992).
- [43] J. P. Lestone, *Phys. Rev. C* **52**, 1118 (1995).
- [44] M. Blann, *Phys. Rev. C* **21**, 1770 (1980).
- [45] J. E. Lynn, *The Theory of Neutron Resonance Reactions* (Clarendon, Oxford, 1968), p. 325.
- [46] V. G. Nedoresov and Y. N. Ranyuk, *Fotodelenie Yader za Gigantskim Rezonansom* (Naukova Dumka, Kiev, 1989) (in Russian).
- [47] R. Vandenbosch and J. R. Huizenga, *Nuclear Fission* (Academic, New York/London, 1973).
- [48] A. Bohr, *Proceedings of the United Nations International Conference on the Peaceful Uses of Atomic Energy* (United Nations, New York, 1956), Vol. 2, p. 151.
- [49] I. Halpern and V. M. Strutinsky, *Proceedings of the United Nations International Conference on the Peaceful Uses of Atomic Energy* (United Nations, Geneva, 1958), Vol. 15, p. 408.
- [50] B. Jurado, C. Schmitt, K.-H. Schmidt, J. Benlliure, T. Enqvist, A. R. Junghans, A. Kelić, and F. Rejmund, *Phys. Rev. Lett.* **93**, 072501 (2004).
- [51] W. Ye, H. W. Yang, and F. Wu, *Phys. Rev. C* **77**, 011302(R) (2008).
- [52] E. Prasad, K. M. Varier, N. Madhavan, S. Nath, J. Gehlot, S. Kalkal, J. Sadhukhan, G. Mohanto, P. Sugathan, A. Jhingan, B. R. S. Babu, T. Varughese, K. S. Golda, B. P. A. Kumar, B. Satheesh, S. Pal, R. Singh, A. K. Sinha, and S. Kailas, *EPJ Web Conf.* **17**, 16011 (2011).
- [53] E. Prasad, K. M. Varier, R. G. Thomas, A. M. Vinodkumar, K. Mahata, S. Appannababu, P. Sugathan, K. S. Golda, B. R. S. Babu, A. Saxena, B. V. John, and S. Kailas, *Nucl. Phys. A* **882**, 62 (2012).
- [54] V. Singh, B. R. Behera, M. Kaur, A. Kumar, K. P. Singh, N. Madhavan, S. Nath, J. Gehlot, G. Mohanto, A. Jhingan, I. Mukul, T. Varughese, J. Sadhukhan, S. Pal, S. Goyal, A. Saxena, S. Santra, and S. Kailas, *Phys. Rev. C* **89**, 024609 (2014).
- [55] K. Mahata, S. Kailas, A. Shrivastava, A. Chatterjee, P. Singh, S. Santra, and B. S. Tomar, *Phys. Rev. C* **65**, 034613 (2002).
- [56] R. Sandal, B. R. Behera, V. Singh, M. Kaur, A. Kumar, G. Singh, K. P. Singh, P. Sugathan, A. Jhingan, K. S. Golda, M. B. Chatterjee, R. K. Bhowmik, S. Kalkal, D. Siwal, S. Goyal, S. Mandal, E. Prasad, K. Mahata, A. Saxena, J. Sadhukhan, and S. Pal, *Phys. Rev. C* **87**, 014604 (2013).
- [57] V. Singh, B. R. Behera, M. Kaur, P. Sugathan, K. S. Golda, A. Jhingan, J. Sadhukhan, D. Siwal, S. Goyal, S. Santra, A. Kumar, R. K. Bhowmik, M. B. Chatterjee, A. Saxena, S. Pal, and S. Kailas, *Phys. Rev. C* **86**, 014609 (2012).
- [58] V. Singh, B. R. Behera, M. Kaur, A. Jhingan, P. Sugathan, S. Pal, D. Siwal, M. Oswal, K. P. Singh, S. Goyal, A. Saxena, and S. Kailas, *EPJ Web Conf.* **86**, 00052 (2015).